Journal of Information Systems Engineering and Management
2025, 10(34s)
e-ISSN: 2468-4376
https://jisem-journal.com/

Research Article

Perclose Image Processing with HRV Signal for Hypnosis Highway Detection

Khusnul Khotimah[1*], Ade Sjafruddin[2], Aine Kusumawati[3], Sony Sulaksono Wibowo[4]

[1] *Ph.D Candidate Of The Faculty Of Civil Engineering, Bandung Institute Of Technology, Bandung City, Indonesia*
[2] *Professor, Faculty Of Civil Engineering, Institute Of Technology Bandung, Bandung City, Indonesia*
[3] *Dr., Associate Professor Of The Faculty Of Civil Engineering, Bandung Institute Of Technology, Bandung City, Indonesia*
[4] *Dr., Associate Professor Of The Faculty Of Civil Engineering, Bandung Institute Of Technology, Bandung City, Indonesia*
* ***Corresponding Author**: khusnulmanisque31@gmail.com*

ARTICLE INFO

Received: 18 Dec 2024

Revised: 10 Feb 2025

Accepted: 28 Feb 2025

ABSTRACT

The driver's hypnosis detection system will be processed by image processing. The background and purpose of this research are to detect street hypnosis and increase street awareness. The road hypnosis detection method is based on eyelid closure and the detection of physiological parameters of the driver's HRV signal to improve the accuracy of detecting the occurrence of hypnosis. This study used the facial landmark method to detect decreased HRV signals related to the driver being asleep or awake. The initial process begins with streaming the camera with a webcam mounted on the vehicle's dashboard. Detection of the facial area uses an eye aspect ratio algorithm that is processed in images captured by a webcam, then an eye ratio algorithm is used to report sleepy eyes in the form of output. The prediction for the first test data is very close to the actual value (0.5567 vs 0.58), which suggests that the model can perform the prediction quite well.

Keywords: Image Processing, HRV Signal, Highway Detection.

INTRODUCTION

Detection of eyelid closure with HRV (Heart Rate Variability) signal interaction is used to monitor the dynamics of stress in drivers, including road hypnosis. Changes in eyelid closure and HRV signals are often associated with the sleep phase and overall sleep quality. The collaboration between the two can establish a real detection of when street hypnosis occurs or the structural pattern of street hypnosis.

National Highway Traffic Safety Administration (NHTSA), United States Department of Transportation [1] recorded a high number of deaths due to drowsiness while driving an average of 846 people over the past 10 years. 16% of fatal accidents are caused by driving fatigue [2].

HSV and MIIR algorithms were developed to realize a robust heart rate estimation system of webcam-based facial color images to detect drowsiness [3]. A sleepiness detection algorithm has been proposed based on eight HRV features of an electrocardiogram (ECG) [4]. This study proposes a sleepiness detection model system to detect simultaneously, using a webcam to cover all levels of sleepiness, from mild hypnosis to severe [5]. Eye position detection is combined with facial images, so drowsiness is assessed based on eye-opening and closing [6]. HRV LF/HF ratio processing is used as an early warning of driver hypnosis [7].

METHODS

Participants

Ten non-smoking male drivers with no history of heart disease, no drugs, and no caffeine were included. They were 35-38 years old and had enough sleep before the driving observation.

Devices

The non-contact method, a photoplethysmographic imaging (PPGI) method using a webcam to receive changes in light, has the advantage of not making the subject feel uncomfortable because there is no contact with the human body [8]. The open and closed eye detection method involves image processing by determining the position of the eyes using the color analysis method and the angle method [9].

In this study, dashboard cameras installed on vehicles are positioned to capture eyelid movements symmetrically and precisely.

Figure 1. Installation and Position of Dashboard Camera on Vehicle

Perclose Data Processing

The given code detects blinks in a video using face detection and eye landmark analysis with MediaPipe and OpenCV. The code also calculates the number of blinks based on the Eye Aspect Ratio (EAR), which detects whether the eyes are closed (blinking) or open. The level of alertness labeling was obtained from the correlation of the HRV signal and the Perclose level.

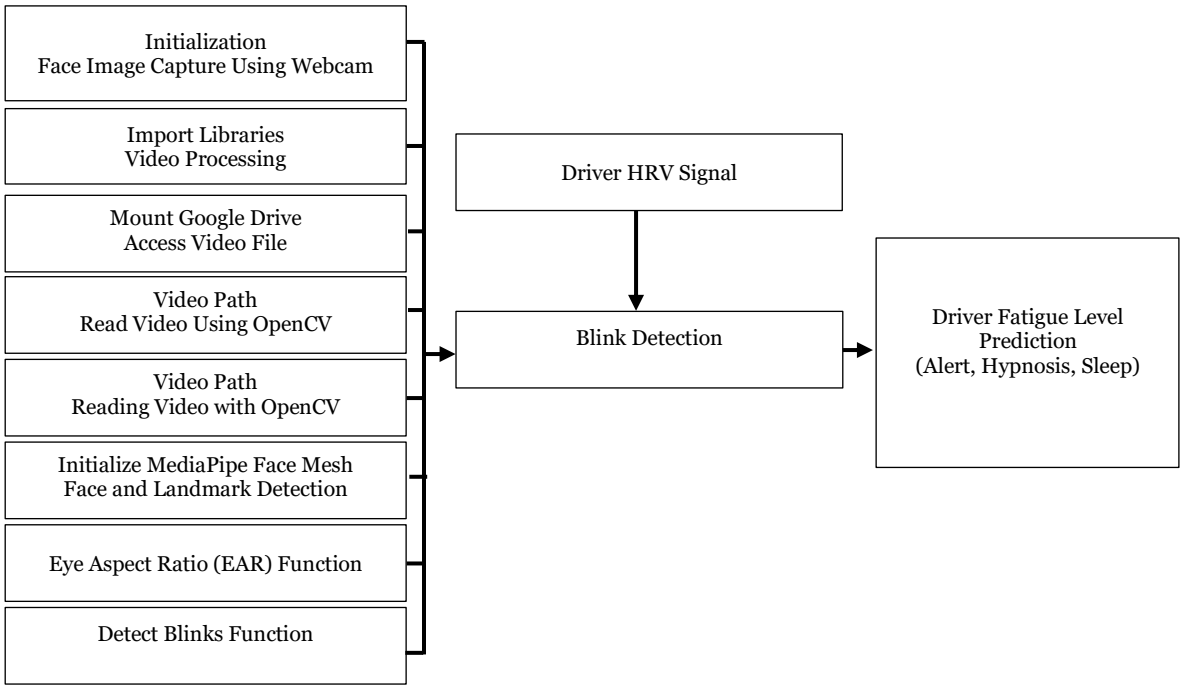

Figure 2. Stages of the Perclose Algorithm

Eye aspect ratio Function (EAR)

This function is used to calculate the Eye Aspect Ratio (EAR), which is the ratio between the vertical (top-bottom) and horizontal (left-right) distances of the eye. The EAR is used to determine whether the eyes are open or closed. If the EAR is low, this indicates shut eyes, which can indicate flickering. A, B, and C are the Euclidean distances between specific points on the eye landmark (e.g., points 1, 2, 5, 6, etc.). The formula calculates EAR:

$$(A + B) / (2.0 * C) \quad (1)$$

Function detect_blinks

This function detects blinks in videos and saves relevant frames. The footage is read using cv2. VideoCapture. The program will issue an error message if the video doesn't open. FaceMesh detects facial landmarks in each video

frame. This landmark finds the eye's position and calculates the EAR.

EAR is calculated for the left and right eyes. If the EAR is less than the threshold (e.g., 0.20), it is considered that the eyes are closed. *EAR_THRESHOLD* is the EAR's lower limit, which is regarded as a sign of closed eyes. At the same time, *EAR_CONSEC_FRAMES* is the number of consecutive frames that must be kept closed to count as a single blink. If the EAR remains low for several successive frames, then this counts as a single wink. Each frame is saved with *a frame_<frame_count>.jpg name for further analysis*.

The detect_blinks function is called to detect flickering in a video for 1 minute (duration = 60 seconds). The number of blinks detected over 1 minute of the video is displayed with print*(f"Number of blinks for 1 minute: {blink_count}")*. Each frame with the detected face landmark is also saved as a jpg image in Google Drive.

When a person enters a state of sleep, the Rapid Eye Movement (REM) cycle begins. When the REM cycle increases to 2, a wave ÿ appears, which can be rated as the point when the driver is completely asleep [10,11,12, 13].

RESULTS

Exploring HRV Signals While Driving

From the results of the recapitulation of heart rate records on all driver samples, a max/min HR of 131/42 bpm, an average HR of 81 bpm for 24 hours, an average HRV (wake/sleep) of 85/76 bpm, a monotonic geometric average HRV of 77-86 bpm, and a geometric fluctuating average HRV of 82-88 bpm. The recorded data shows that when driving, HRV tends to decrease from average to sleep mode [14,15,16,17].

(a)

(b)

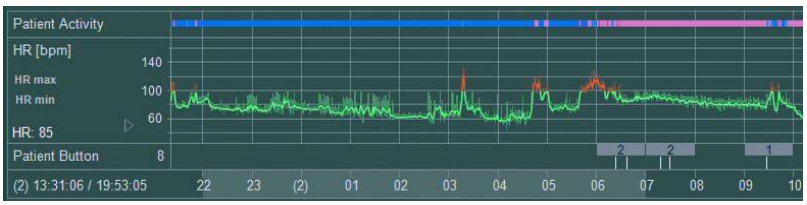

(c)

Figure 3. HRV Interaction While Driving in Monotonous Road Conditions, (a) At the beginning of departure, (b) At the end of the trip, (c) For 24 Hours

RR (ms), QT (ms), and PQ (ms) data were obtained from the recording of Holter monitor data for 24 hours. This data produces an analysis of the dominance of the driver's autonomic nerve in every activity carried out by the driver [18,19]

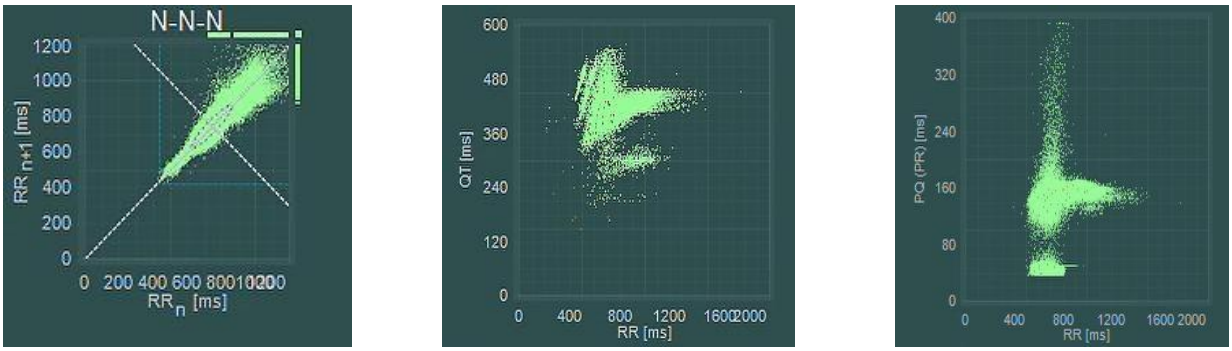

Figure 4. Conditions of (a) RR Signal, (b) QT Signal, (c) PQ Signal in Driver

In Figure 4(a), the RR interval is shorter. This condition interprets that when a person is in a state of stress, the heart rate becomes faster, which causes the RR interval between successive heartbeats to be shorter [20,21,22]. The QT interval is shorter (Fig.4(b)). In mild or short-term stress, some studies suggest that adrenaline can decrease the duration of the QT interval, possibly due to a rapid increase in heart rate (shorter time between heartbeats). It is the body's response to stress, which allows the heart to adapt quickly to changes. PR/PQ interval figure 4(c), decreased heart rate variability (HRV), interprets the activation of the sympathetic nervous system due to stress. This condition can cause an increase in heart rate accompanied by decreased heart rate variability (HRV). This condition shortens the PR interval on the ECG. When the sympathetic nervous system predominates, the speed of conduction of electrical impulses from the atria to the ventricles can increase, which causes shorter PR intervals so that alertness decreases [23,24,25].

Table 1. Analysis of Driver's Autonomous Neural Dominance on Sleep and Driving Conditions

Condition	Time	SDNN	LF/HF	LF	HF	RMSSD	HRV	Parameter
Sleep	01.00 AM	115	0,92	0,61	0,67	71	70	Parasympathetic
Sleep	02.00 AM	109	0,77	0,51	0,67	78	65	Parasympathetic
Sleep	03.00 AM	154	1,02	0,51	0,5	56	72	Parasympathetic
Mean of Sleep		105	0,86	0,51	0,60	63	72	Parasympathetic
Monotonous Road Driving	07.00 AM	43	1,27	0,29	0,23	23	88	Sympathetic
Monotonous Road Driving	08.00 AM	50	1,37	0,36	0,26	29	81	Sympathetic
Monotonous Road Driving	09.00 AM	75	1,18	0,31	0,27	31	82	Sympathetic
The Mean of Monotonous Road Driving		56	1,27	0,32	0,25	27,67	84	Sympathetic

A decrease in SDNN from RR data processing of more than 5% % to 15% can indicate that the driver has begun to enter a hypnotic state (with sympathetic dominance) [26,27,28].

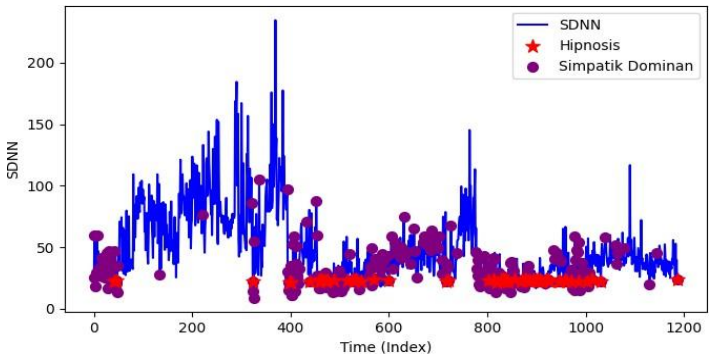

Figure 5. Driver hypnosis in the SDNN ratio change during driving

Perclose

Observing drivers while driving revealed a decrease in HRV. However, a reduction in HRV does not cause HRV in any noticeable sleep conditions.

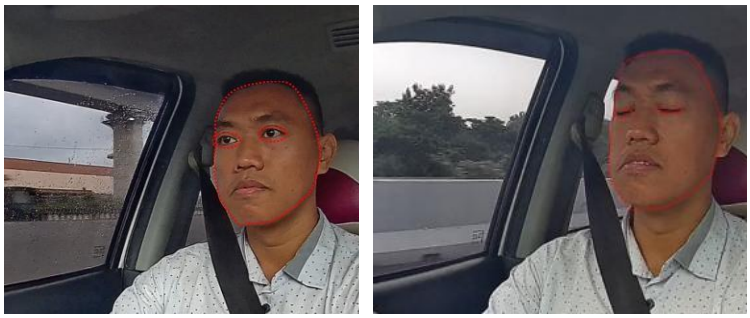

(a) (b)

Figure 6. Blink Detection, (a) Eyes Open Detection, (b) Eyes Closed Detection

Figure 7. Blink Detection EAR Results

Perclose Model Development

The model is built using the Hard Sequential API. First, an LSTM layer is added with 50 units (neurons). This layer will process the given time series data. A dropout layer was added to prevent overfitting. Then, a Dense layer is added to produce a single prediction output (value Perclos (%). The model is compiled using the Adam optimizer and the loss function mean_squared_error.

	HRV_(bpm)	Number_of_flickers	Duration_of_flickers_(Seconds)	Perclos (%)
0	99.009901	25	7.5	0.125
1	95.846645	44	13.2	0.220
2	98.684211	55	16.5	0.275
3	99.667774	43	12.9	0.215
4	98.360656	49	14.7	0.245

	Fatigue Level
0	0
1	0
2	0
3	0
4	0

The training model was trained using training data, with the number of epochs specified as 20 and batch_size 32.

Epoch 1/20

/usr/local/lib/python3.11/dist-packages/keras/src/layers/rnn/rnn.py:200: UserWarning: Do not pass an `input_shape`/`input_dim` argument to a layer. When using Sequential models, I prefer using an `Input(shape)` object as the first layer in the model instead.'

super().__init__(**kwargs)

5/5 ━━━━━━━━━━━━━━━━━━━━ **5s** 14ms/stop - loss: 0.2046 Epoch 2/20

5/5 ━━━━━━━━━━━━━━━━━━━━ **0s** 13ms/stop - loss: 0.1790 Epoch 3/20

5/5 ━━━━━━━━━━━━━━━━━━━━ **0s** 18ms/stop - loss: 0.1547 Epoch 4/20

5/5 ━━━━━━━━━━━━━━━━━━━━ **0s** 11ms/stop - loss: 0.1337 Epoch 5/20

5/5 ━━━━━━━━━━━━━━━━━━━━ **0s** 12ms/stop - loss: 0.1164 Epoch 6/20

5/5 ━━━━━━━━━━━━━━━━━━━━ **0s** 12ms/stop - loss: 0.1067 Epoch 7/20

5/5 ━━━━━━━━━━━━━━━━━━━━ **0s** 19ms/stop - loss: 0.0854 Epoch 8/20

5/5 ━━━━━━━━━━━━━━━━━━━━ **0s** 16ms/stop - loss: 0.0751 Epoch 9/20

5/5 ━━━━━━━━━━━━━━━━━━━━ **0s** 11ms/stop - loss: 0.0587 Epoch 10/20

5/5 ━━━━━━━━━━━━━━━━━━━━ **0s** 14ms/stop - loss: 0.0505 Epoch 11/20

5/5 ━━━━━━━━━━━━━━━━━━━━ **0s** 12ms/stop - loss: 0.0415 Epoch 12/20

5/5 ━━━━━━━━━━━━━━━━━━━━ **0s** 40ms/stop - loss: 0.0362 Epoch 13/20

5/5 ━━━━━━━━━━━━━━━━━━━━ **0s** 23ms/stop - loss: 0.0273 Epoch 14/20

5/5 ━━━━━━━━━━━━━━━━━━━━ **0s** 29ms/stop - loss: 0.0208 Epoch 15/20

5/5 ━━━━━━━━━━━━━━━━━━━━ **0s** 21ms/stop - loss: 0.0207 Epoch 16/20

5/5 ━━━━━━━━━━━━━━━━━━━━ **0s** 26ms/stop - loss: 0.0170 Epoch

```
17/20
5/5 ━━━━━━━━━━━━━━━━━━━━━━━━━━━━━━━━━━━━ 0s 8ms/stop - loss: 0.0151 Epoch
18/20
5/5 ━━━━━━━━━━━━━━━━━━━━━━━━━━━━━━━━━━━━ 0s 8ms/stop - loss: 0.0150 Epoch
19/20
5/5 ━━━━━━━━━━━━━━━━━━━━━━━━━━━━━━━━━━━━ 0s 8ms/stop - loss: 0.0138 Epoch
20/20
5/5 ━━━━━━━━━━━━━━━━━━━━━━━━━━━━━━━━━━━━ 0s 8ms/stop - loss: 0.0161
2/2 ━━━━━━━━━━━━━━━━━━━━━━━━━━━━━━━━━━━━ 0s 175ms/step
```

MODEL RESULTS

After training, the model predicts the Perclos (%) value on the test data, and the expected value is returned to the original scale. The Mean Squared Error (MSE) and R-squared metrics evaluate the model's performance.

LSTM Model Results		
First Prediction	=	0.5567
Actual First	=	0.58
Mean Squared Error (MSE)	=	0.011796681997537337
R-squared	=	0.6027523855338464

The model predicts that the Perclos (%) for the first test data example is around 0.5567. This value is already normalized to the range [0, 1] because we use a MinMaxScaler on the target. The actual Perclos value (%) (original target value) in the first test data was about 0.58. This value has also been normalized. Mean Squared Error (MSE) 0.011796681997537337. A low MSE value indicates that the model did not make significant prediction errors, with several 0.0118 indicating that the model performed exceptionally well. The smaller the MSE, the better the model's predictions compare to the actual value. R-squared (R^2) measures how well the model describes variations in the target data. The R^2 value ranges from 0 to 1. Your R^2 value is about 0.6027; the model explains about 60.27% of the variation in the Perclos (%). This shows that the model is pretty good at predicting Perclos (%), although there is room for improvement.

Prediction and Actual Plotting to see how close the prediction is to the actual value can be seen in the following diagram:

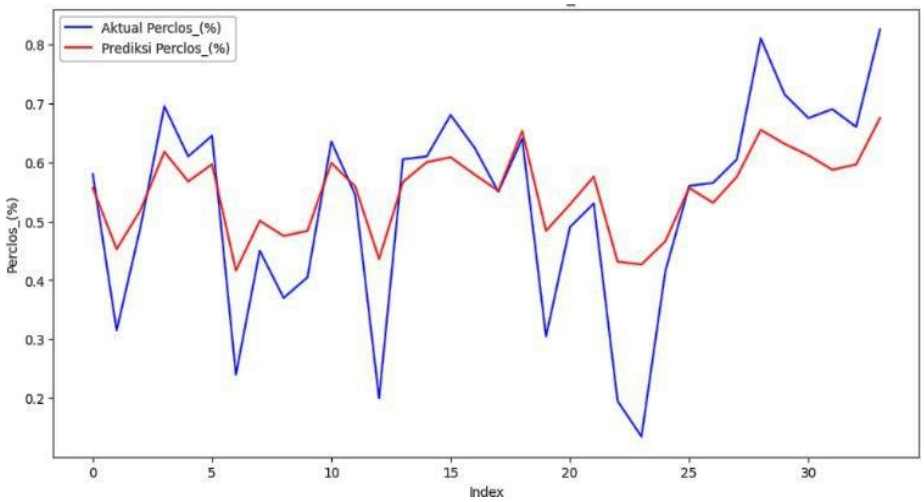

Figure 8. Plotting Prediction and Actual Perclose (%)

Loss Curve during training to monitor whether the model is converging and to verify if overfitting occurs. The loss curve visualization can be seen as follows:

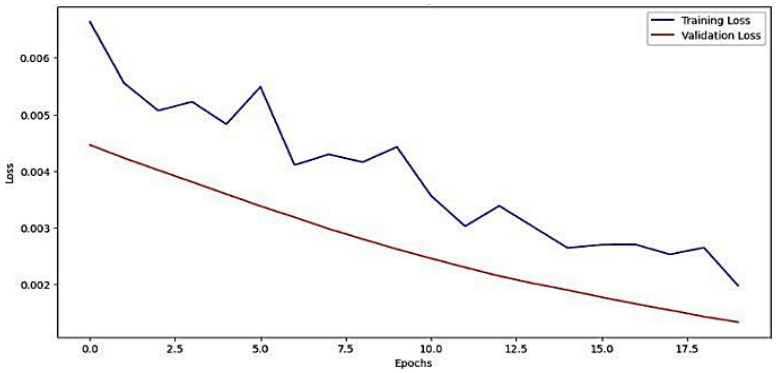

Figure 9. Loss Curve Training Vs. Validation

CONCLUSION

The prediction for the first test data is very close to the actual value (0.5567 vs 0.58), which indicates that the model can perform predictions quite well. A small MSE suggests that the model error is relatively low. An R^2 of about 0.60 indicates that the model explains most of the variation in the data, but there are about 40% of the variations that the model cannot yet explain. This can mean that other factors affect Perclos (%) that are not accommodated by the features used in the model (such as HRV, number of blinks, and blink duration). In the subsequent assessment, a combination of road environmental conditions can be further investigated to assess the level of hypnosis and the performance of the road system.

ACKNOWLEDGMENTS, SUPPORT, AND FUNDING

This research is supported by the Education Fund Management Institution, Ministry of Finance (SKPB-3349/LPDP/LPDP.3, 2023); Directorate of Traffic and Road Transportation, Ministry of Transportation (B.427, 2024); BTL Medical Center Indonesia (745, 2024).

REFRENCES

[1] National Highway Traffic Safety Administration (NHTSA). Online, 1 July 2017: http://www.nhtsa.gov
[2] Nordbakke, S.; Sagberg, F. Drowsiness While Driving: Knowledge, Symptoms And 51 Car Driver Behaviors. Trans. Res. Part F **2007,** 10, 1–10. https://doi.org/10.1016/j.trf.2006.03.003
[3] Cho, D.; Lee, B. Non-contact strong heart rate estimation using HSV color model and matrix-based IIR filters in facial video imaging. In the Proceedings of the 38th Annual International Conference of the IEEE Engineering in Medicine and Biology Society (EMBC), Orlando, FL, AS, August 16–20, 2016; pp.3847–3850.
[4] Fujiwara, K.; Tawon.; Kamata, K.; Nakayama, C.; Suzuki, Y.; Yamakawa, T.; Hiraoka, T.; Kano, M.; Sumi, Y.; Masuda, F.; dkk. Detection of driver sleepiness based on heart rate variability and its validation with EEG. IEEE Trans. Bioma. English 2019, 66, 1769–1778, [Cross-references], https://doi.org/10.1109/TBME.2018.2879346
[5] Sunagawa, M.; Shikii, SI; Nakai, W.; Mochizuki, M.; Kusukame, K.; Kitajima, H. Deteksi tingkat kantuk yang komprehensif model yang menggabungkan informasi multimodal. Sensasi IEEE J. 2020, 20, 3709–3717. https://doi.org/10.1109/JSEN.2019.2960158
[6] Chang, C.W., Hough, D., Drowsy Driver Detection System Transformation and Embedded System Implementation. Master's Thesis, Nat. Chung Hsing University, Taichung, Taiwan, 2014.
[7] Chang, RC-H.; Wang, C.-Y.; Kao, Y.-Y; Implementation of a new intelligent sleep-detection alert system. In the Proceedings of the 2021 IEEE International Conference on Consumer Electronics, Penghu, Taiwan, September 15–17, 2021.
[8] Guo, BN; Lin, CY; Study of vital signs measured using a webcam. JITA 2012, 6, 112–118. [9.] Park, I.; Ahn, J.-H.; Byun, H. Efficient measurement of blinking in various lighting conditions for sleepiness detection systems. In ICPR Proceedings 2006—18th International Conference on Pattern Recognition, Hong Kong, 20–24 August 2006; pp.383–386.
[9] Szypulska, M.; Piotrowski, Z. Predict fatigue and sleep onset using HRV analysis. In the Proceedings of the 19th International Conference on Mixed Design of Circuits and Integrated Systems-MIXDES 2012, Warsaw, Poland, 24–26 May 2012; pp. 543–546.

[10] J. Thiffault, P.; Bergeron, "Monotony of road environment and driver fatigue: A simulator study," *Accid. Anal. Prev.*, vol. 35, no. 3, pp. 381–391, 2003, doi: https://doi.org/10.1016/S0001-4575(02)00014-3
[11] D. Gershon, P.; Ronen, A.; Oron-Gilad, T.; Shinar, "The effects of an interactive cognitive task (ICT) in suppressing fatigue symptoms in driving," *Transp. Res. Part F Traffic Psychol. Behav.*, vol. 12, no. 1, pp. 21–28, 2009, doi: https://doi.org/10.1016/j.trf.2008.06.004.
[12] M.-C. Ting, P.-H.; Hwang, J.-R.; Doong, J.-L.; Jeng, "Driver fatigue and highway driving: A simulator study," *Physiol. Behav.*, vol. 94, no. 3, pp. 448–453, 2008, doi: https://doi.org/10.1016/j.physbeh.2008.02.015.
[13] R. J. Javid, R. Jahanbakhsh Javid, "A framework for travel time variability analysis using urban traffic incident data," *IATSS Res.*, vol. 42, no. 1, pp. 30–38, 2018, doi: https://doi.org/10.1016/j.iatssr.2017.06.003.
[14] R. Orsini, F.; Giusti, G.; Zarantonello, L.; Costa, R.; Montagnese, S.; Rossi, "Driving fatigue increases after the Spring transition to Daylight Saving Time in young male drivers: A pilot study," *Transp. Res. Part F Traffic Psychol. Behav.*, vol. 99, pp. 83–97, 2023, doi: https://doi.org/10.1016/j.trf.2023.10.014.
[15] A. H. Wertheim, "Explaining highway hypnosis: Experimental evidence for the role of eye movements," *Accid. Anal. Prev.*, vol. 10, no. 2, pp. 111–129, 1978, doi: https://doi.org/10.1016/0001-4575(78)90019-2.
[16] M. J. Cerezuela, G.P.; Tejero, P.; Chóliz, M.; Chisvert, M.; Monteagudo, "Wertheim's hypothesis on 'highway hypnosis': Empirical evidence from a study on motorway and conventional road driving," *Accid. Anal. Prev.*, vol. 36, no. 6, pp. 1045–1054, 2004, doi: https://doi.org/10.1016/j.aap.2004.02.002.
[17] F. Shi, H.; Chen, L.; Wang, X.; Wang, B.; Wang, G.; Zhong, "Research on Recognition of Road Hypnosis in the Typical Monotonous Scene," *Sensors*, vol. 23, no. 3, 2023, doi: https://doi.org/10.3390/s23031701.
[18] J.-L. Jacobé de Naurois, C.; Bourdin, C.; Stratulat, A.; Diaz, E.; Vercher, "Detection and prediction of driver drowsiness using artificial neural network models," *Accid. Anal. Prev.*, vol. 126, pp. 95–104, 2019, doi: https://doi.org/10.1016/j.aap.2017.11.038.
[19] M. Fujiwara, K.; Abe, E.; Kamata, K.; Nakayama, C.; Suzuki, Y.; Yamakawa, T.; Hiraoka, T.; Kano, "Heart Rate Variability-Based Driver Drowsiness Detection and Its Validation With EEG," *IEEE Trans. Biomed. Eng.*, vol. 66, no. 6, pp. 1769–1778, 2019, doi: https://doi.org/10.1109/TBME.2018.2879346.
[20] V. Jagannath, M.; Balasubramanian, "Assessment of early onset of driver fatigue using multimodal fatigue measures in a static simulator," *Appl. Ergon*, vol. 45, no. 4, pp. 1140–1147, 2014, doi: https://doi.org/10.1016/j.apergo.2014.02.001.
[21] M. Awais, M.; Badruddin, N.; Drieberg, "A hybrid approach to detect driver drowsiness utilizing physiological signals to improve system performance and Wearability," *Sensors (Switzerland)*, vol. 17, no. 9, 2017, doi: https://doi.org/10.3390/s17091991.
[22] P. Jap, B.T.; Lal, S.; Fischer, "Comparing combinations of EEG activity in train drivers during monotonous driving," *Expert Syst. Appl.*, vol. 38, no. 1, pp. 996–1003, 2011, doi: https://doi.org/10.1016/j.eswa.2010.07.109.
[23] H. C. Ahn, J.W.; Ku, Y.; Kim, "A novel wearable EEG and ECG recording system for stress assessment," *Sensors (Switzerland)*, vol. 19, no. 9, 2019, doi: https://doi.org/10.3390/s19091991.
[24] M. Vogelpohl, T.; Kühn, M.; Hummel, T.; Vollrath, "Asleep at the automated wheel—Sleepiness and fatigue during highly automated driving," *Accid. Anal. Prev.*, vol. 126, pp. 70–84, 2019, doi: https://doi.org/10.1016/j.aap.2018.03.013.
[25] M. Sauvet, F.; Bougard, C.; Coroenne, M.; Lely, L.; Van Beers, P.; Elbaz, M.; Guillard, M.; Léger, D.; Chennaoui, "In-flight automatic detection of vigilance states using a single EEG channel," *IEEE Trans. Biomed. Eng.*, vol. 61, no. 12, pp. 2840–2847, 2014, doi: https://doi.org/10.1109/TBME.2014.2331189.
[26] A. M. Farahmand, B.; Boroujerdian, "Effect of road geometry on driver fatigue in monotonous environments: A simulator study," *Transp. Res. Part F Traffic Psychol. Behav.*, vol. 58, pp. 640–651, 2018, doi: https://doi.org/10.1016/j.trf.2018.06.021.
[27] T.-J. Liu, Y.-C.; Wu, "Fatigued driver's driving behavior and cognitive task performance: Effects of road environments and environment changes," *Saf. Sci.*, vol. 47, no. 8, pp. 1083–1089, 2009, doi: https://doi.org/10.1016/j.ssci.2008.11.009.
[28] L. Zhou, F.; Alsaid, A.; Blommer, M.; Curry, R.; Swaminathan, R.; Kochhar, D.; Talamonti, W.; Tijerina, "Driver fatigue transition prediction in highly automated driving using physiological features," *Expert Syst. Appl.*, vol. 147, 2020, doi: https://doi.org/10.1016/j.eswa.2020.113204.